AIAA JOURNAL
Vol. 30, No. 7, July 1992

Study of Turbulence on Supersonic Compression Surfaces Using Reynolds Stress Model

J. Lee* and D. B. Taulbee†
State University of New York at Buffalo, Buffalo, New York 14260
and
M. S. Holden‡
Calspan-University at Buffalo Research Center, Buffalo, New York 14225

A theoretical study was conducted to determine the effects of adverse pressure gradient and compressibility in modeling turbulent compressible flows. The zero equation, kinetic-energy/dissipation eddy-viscosity models, and Reynolds stress model predictions are presented and compared with experimental data. It is shown that the effects of compressibility, which include the mass-averaged fluctuation term $\overline{u_j''}$, the pressure-dilatation term $\overline{p'\partial u_l''/\partial x_l}$, and the dilatation dissipation $\overline{\mu(\partial u_l''/\partial x_l)^2/\bar{\rho}}$, are important in modeling turbulent compressible flows. It is also shown that the normal stresses and longitudinal strain rates have an effect in the prediction of turbulent energy production on curved compression ramps. A new compressible formulation of the pressure-strain term, which includes the effects of the normal-stress/mean-dilatation interactions, in the Reynolds stress equation is presented. The boundary-layer forms of the kinetic-energy/dissipation and Reynolds stress models were used in this study. Mass (Favre)-averaged Navier-Stokes equations and zero-equation eddy viscosity were also employed to assess possible limitations of the boundary-layer approximations used for the compression-surface problems considered in this study.

Nomenclature

D_{ij} = $\bar{\rho}\tau_{ik}\partial\tilde{U}_k/\partial x_j + \bar{\rho}\tau_{jk}\partial\tilde{U}_k/\partial x_i$
$\tilde{k}$ = Favre-averaged turbulent kinetic energy, $\overline{\rho u_l'' u_l''}/2\bar{\rho}$
l = surface distance of compression surface
M_t = turbulent Mach number, $\sqrt{\tau_{ll}/\gamma R\bar{T}}$
P = $P_{ll}/2$
R = gas constant
R_c = radius of curvature
R_t = turbulent Reynolds number, $\tilde{k}^2/\tilde{\epsilon}\nu$
T = temperature
U = velocity
U_τ = friction velocity, $\sqrt{\tau_w/\rho_w}$
y^+ = normalized wall distance, yU_τ/ν_w
ϵ = total dissipation away from the wall
ϵ_d = dilatation dissipation, $\overline{\mu(\partial u_l''/\partial x_l)^2}/\bar{\rho}$
ϵ_{ij} = total dissipation
$\tilde{\epsilon}$ = solenoidal dissipation, $\overline{\mu(\partial u_i''/\partial x_l)^2}/\bar{\rho}$
δ = boundary-layer thickness
δ_{ij} = Kronecker delta
γ = specific heat ratio = 1.4
μ = viscosity
μ_t = eddy viscosity, $C_\mu\tilde{k}^2/\tilde{\epsilon}$
σ_{ij} = total viscous stresses
τ_{ij} = Favre-averaged Reynolds stresses, $\overline{\rho u_i'' u_j''}/\bar{\rho}$

Subscripts

e = at edge
w = at wall
∞ = at freestream
0 = stagnation value

Superscripts

$\sim$ = Favre-averaged quantity
$-$ = Reynolds-averaged quantity
$''$ = mass fluctuations
$'$ = fluctuations

Introduction

In the past several years, significant progress has been made in computational fluid dynamics (CFD) for simulating high-speed flows. Major progress has been made in development and understanding of the numerical aspects of CFD. However, further development and understanding of physical models (e.g., turbulence models, chemistry models) are required if CFD is to reach its full maturity. Because of practical limitations imposed by the size of the computer, the role played by turbulence modeling is of fundamental importance in the prediction of high-speed flows. In the present work, the modeling of turbulence in high-Mach-number flows with adverse pressure gradients is addressed.

The closure of the turbulent Reynolds stresses required for these problems can be accomplished with eddy-viscosity (including the k-ϵ model) and Reynolds stress models. Most of the calculations to date have made use of k-ϵ and other lower-order eddy-viscosity turbulence models to predict complex turbulent shock-wave/boundary-layer interactions, and a number of potential weaknesses of these models have been exposed (Marvin[1]). Zero-equation models, such as that of Baldwin-Lomax,[2] have limited applicability in complex separated-flow situations, because of the universal near-wall length scale formulation used. In principle, the k-ϵ model is more general and has been used with limited success in predicting three-dimensional flows, including shock-wave/boundary-layer interactions. The k-ϵ models, however, have a weakness

Presented as Paper 90-1592 at the AIAA 21st Fluid and Plasma Dynamics Conference, Seattle, WA, June 18-20, 1990; received July 10, 1991; revision received Oct. 23, 1991; accepted for publication Oct. 23, 1991. Copyright © 1992 by the American Institute of Aeronautics and Astronautics, Inc. All rights reserved.

*CFD Research Scientist; currently at Sverdrup Technology, NASA Lewis Group, 2001 AeroSpace Parkway, Brook Park, OH, 44142. Member AIAA.

†Professor, Department of Mechanical and Aerospace Engineering. Associate Fellow AIAA.

‡Staff Scientist, P.O. Box 400. Associate Fellow AIAA.

in resolving the normal stresses and, consequently, result in poor predictions of the production and pressure/strain processes of turbulence.

The k-ϵ model utilizes a turbulent stress/strain relationship analogous to the laminar stress/strain formulation (Boussinesq formulation). This relationship implies that the Reynolds stress tensor is aligned with the mean strain rates. In nearly parallel flows, this stress/strain relationship is a good approximation for the shear stress; thus, the k-ϵ model is a useful predictive tool. Even in some more general multidimensional flow situations, the k-ϵ model will give an adequate prediction. However, due to the stress/strain relationship employed, the accuracy in the normal Reynolds stress predictions is mostly lost in the k-ϵ predictions. This weakness could also cause the k-ϵ model to give poor predictions of bulk dilatation-dominated flows, such as the shock-wave/boundary-layer interaction and compression-surface flows. Therefore, a more accurate model should be used in flows where large normal stresses and large dilatational effects are present, as in the supersonic turbulent flow over a compression ramp.

The Reynolds stress model uses the dynamic equations for the Reynolds stresses and is, therefore, more general than the k-ϵ model, in which the stresses are given by the local constitutive relationship. Also, the Reynolds stress model can be formulated so that ad hoc corrections are not required to model the effects of curvature.[3] Previous calculations of compressible turbulent flows with adverse pressure-gradient effects using a second-order closure are limited in number, and most of the work to date has concentrated on the computation of shock-wave/boundary-layer interactions.[4-6] Marvin[1] summarizes the computations made using the Reynolds stress models of Wilcox and Rubesin[7] and Donaldson and Sullivan.[8] Figure 4 of Marvin[1] illustrates that the performance of the Reynolds stress models is superior to that of the algebraic eddy-viscosity models in the adverse pressure-gradient regions.

Modeling of compressibility effects is also important in high-Mach-number flows. Horstman[5] has shown that pressure-dilatation effects and mass-averaged velocity terms cannot be neglected in predicting the flow over wedge compression surfaces. Recently, Zeman[9] and Sarkar et al.[10] have shown that the solenoidal dissipation normally used in these calculations is inadequate, because it represents only a part of the total dissipation process. Zeman and Sarkar et al. proposed that dilatation dissipation, which they formulated as a function of the turbulent Mach number, should be included in the turbulent compressible flow predictions.

We chose curved-ramp configurations in supersonic flows to study the influence of the strain field and the compressibility terms without the added complexity caused by the shock-wave/boundary-layer interactions. Comprehensive data for the curved compression surface with an initial Mach number of 2.87 are given by Degani and Smits,[11] Jarayam et al.,[12] and Sturek and Danberg.[13] For prediction purposes, the curved compression ramp has an advantage over the sharp corner; since the compression process occurs over a distance of the curved surface, rather then at a sharp corner, a much milder pressure-gradient level is achieved, and the turbulent production level can be controlled by changing the curvature. Hence, for large-curvature configurations, there is no separation, and the flow can be adequately described by the boundary-layer approximation.

The present investigation pursued the subject of modeling these compressibility effects though the use of the Favre (mass)-averaged[14] Reynolds stress model. The Launder et al.[17] formulation of the Reynolds stress model was modified to include the effects of the pressure-dilatation, the dilatation-dissipation, and the mass-averaged fluctuations. This second-order closure model was then used to investigate the role that the normal stresses and strain rates play in the production of turbulence in Mach 2.87 flow though an adverse pressure gradient. The predictions of the Reynolds stress models were also compared with the k-ϵ model predictions to illustrate the potential weakness of the k-ϵ models. The possible limitations of the boundary-layer formulation of these models were also explored through the use of full mass-averaged Navier-Stokes equations with a zero-equation eddy-viscosity model.

Theory

Kinetic-Energy/Dissipation Model

The mass-averaged form of the Chien[15] k-ϵ model was used in our investigation. This model was chosen because it gave the best prediction of the flat-plate boundary layer. In two-equation models, the required length scales are calculated in terms of the turbulent flowfield. However, two-equation models also have inherent defects in that the effects of the normal strain rates have been incorporated into the model through the use of the constitutive relation. The constitutive relation, given by,

$$-\bar{\rho}\tau_{ij} = \mu_t\left(\frac{\partial \tilde{U}_i}{\partial x_j} + \frac{\partial \tilde{U}_j}{\partial x_i} - \frac{2}{3}\delta_{ij}\frac{\partial \tilde{U}_k}{\partial x_k}\right) - \frac{2}{3}\bar{\rho}\tilde{k}\delta_{ij} \tag{1}$$

is used to determine the Reynolds stresses. This relationship performs well for the shear component, but the normal components are not accurately predicted in many flows. In a simple case of homogeneous shear flow, where $U = U(y)$, the above equation yields the isotropic relationship, $\tau_{xx} = \tau_{yy} = \tau_{zz} = 2/3\tilde{k}$. This is not consistent with the experimental observations, even though the relationship for the shear component, $-\bar{\rho}\tau_{xy} = \mu_t \partial\tilde{U}/\partial y$, is satisfied. If the flow is shear dominated, turbulence models using Eq. (1) will yield reasonable predictions of the flow. Using these models to predict flows that are normal-stress dominated could result in error, since the incorrectly predicted normal stresses will lead to incorrect prediction of the turbulent kinetic energy production. An illustration of this weakness was given by Taulbee,[16] who showed that stagnation streamline turbulence, which is dominated by normal stresses along with normal strain rates, is incorrectly predicted by the standard k-ϵ model.

Reynolds Stress Model

To overcome these difficulties of the k-ϵ model, the mass-averaged Reynolds stress model was adopted for the present study. The mass-averaging process yields transport equations that are term-by-term identical to the Reynolds-averaged transport equations with the exception of the terms involving viscosity and density.

The dynamic equations of Reynolds stress τ_{ij} in mass-averaged variables are given by

$$\frac{\mathrm{D}}{\mathrm{D}t}(\bar{\rho}\tau_{ij}) = -\frac{\partial}{\partial x_k}(C_{ijk} - D_{ijk} + E_{ijk}) - P_{ij} + \Phi_{ij} - MA_{ijk} - \epsilon_{ij} \tag{2}$$

where

Turbulent flux:

$$C_{ijk} = \overline{\rho u_i'' u_j'' u_k''} \tag{3}$$

Viscous diffusion:

$$D_{ijk} = \overline{\sigma_{ik}'' u_j''} + \overline{\sigma_{jk} u_i''} \tag{4}$$

Pressure diffusion:

$$E_{ijk} = \overline{p' u_j''}\,\delta_{ik} + \overline{p' u_i''}\,\delta_{jk} \tag{5}$$

Pressure strain:

$$\Phi_{ij} = \overline{p'\left(\frac{\partial u_i''}{\partial x_j} + \frac{\partial u_j''}{\partial x_i}\right)} \tag{6}$$

Total dissipation:

$$\epsilon_{ij} = \overline{\sigma''_{ik} \frac{\partial u''_j}{\partial x_k}} + \overline{\sigma''_{jk} \frac{\partial u''_i}{\partial x_k}} \tag{7}$$

Production:

$$P_{ij} = \bar{\rho}\tau_{ik} \frac{\partial \tilde{U}_j}{\partial x_k} + \bar{\rho}\tau_{jk} \frac{\partial \tilde{U}_i}{\partial x_k} \tag{8}$$

Mass-averaged terms:

$$MA_{ijk} = \overline{u''_i}\left(\frac{\partial \bar{p}}{\partial x_j} - \frac{\partial}{\partial x_k}\tilde{\sigma}_{jk}\right) + \overline{u''_j}\left(\frac{\partial \bar{p}}{\partial x_i} - \frac{\partial}{\partial x_k}\tilde{\sigma}_{ik}\right) \tag{9}$$

The Reynolds stress model of Launder et al.[17] has proven to work reasonably well in predicting many different types of high-Reynolds-number flows. An update to their earlier model to account for the viscous diffusion and wall effects of pressure/strain was proposed by Hanjalic and Launder.[18] The Reynolds stress model used in this study of the supersonic turbulent boundary layer over an adverse pressure gradient was developed from these two model formulations. The model formulations for the turbulent flux, the viscous-diffusion, and the near-wall total dissipation in mass-averaged variables are given by the following:

The turbulent-flux (including pressure-diffusion) terms are

$$C_{ijk} = -C_s\bar{\rho}\frac{\tilde{k}}{\tilde{\epsilon}}\left(\tau_{kl}\frac{\partial}{\partial x_l}\tau_{ij} + \tau_{jl}\frac{\partial}{\partial x_l}\tau_{ki} + \tau_{il}\frac{\partial}{\partial x_l}\tau_{jk}\right) \tag{10}$$

The viscous-diffusion terms are approximated by

$$D_{ijk} = \bar{\mu}\left(\frac{\partial}{\partial x_k}\tau_{ij}\right) \tag{11}$$

The total-dissipation terms are

$$\epsilon_{ij} = \frac{\epsilon}{\tilde{k}}\left(\bar{\rho}\tau_{ij}f_s + \frac{2}{3}(1-f_s)\bar{\rho}\tilde{k}\delta_{ij}\right) \tag{12}$$

where C_s is set to 0.11 as suggested by Launder et al.[17] and the wall function f_s is equal to $10/(10 + R_t)$.

Pressure/Strain Model

The basic closure of the pressure/strain term appearing in the dynamic equations for incompressible flow was proposed by Launder et al.[17] However, it cannot be assumed that this formulation can be carried over to compressible flows. In incompressible flow, the trace of the pressure/strain correlation must vanish to satisfy continuity. This leads to the conclusion that the pressure/strain process involves only turbulent energy redistribution in incompressible flows. For compressible flow, however, the density appears in the Poisson equation for the pressure fluctuation; consequently, the trace of the pressure/strain correlation may not vanish and, therefore, is no longer just an energy redistribution term. Ha-Minh et al.,[19] Cousteix and Aupoix,[20] and Strahle[21] recommended modifications of the rapid term in the pressure/strain formulation in which the trace of the models vanishes. We have re-examined the formulation of the closure for the rapid part of the pressure/strain term, since the trace pressure/strain may not vanish because of the additional strain field generated by the variable density.

The pressure/strain term is formulated from the Poisson equation for pressure fluctuations, neglecting viscous effects,

$$\frac{\partial^2 p'}{\partial x_i^2} = \frac{\partial^2 \rho'}{\partial t^2} - \frac{\partial^2}{\partial x_l \partial x_k}(\rho' \tilde{U}_l \tilde{U}_k) + \frac{\partial^2}{\partial x_l \partial x_k}(2\tilde{U}_l \rho u''_k + \rho u''_l u''_k - \overline{\rho u''_l u''_k}) \tag{13}$$

The first term on the right side of Eq. (13) accounts for unsteady acoustic-wave propagation. This term is neglected at the present time, since it is assumed that the turbulent pressure fluctuations are associated primarily with the local-source terms. The second term on the right side of Eq. (13) arises from the density fluctuations. This term is also neglected for the present analysis of the supersonic turbulent boundary layers. We are then left with a Poisson equation that is analogous to the incompressible form except for the appearance of variable density. Equation (13) consists of the slow term, which represents the turbulent/turbulent interactions, and the rapid term, which represents the turbulent/mean interaction.

The linear-return-to-isotropy model,

$$\Phi_{ij,1} = -C_1\bar{\rho}\frac{\tilde{\epsilon}}{\tilde{k}}\left(\tau_{ij} - \frac{2}{3}\tilde{k}\delta_{ij}\right) \tag{14}$$

originally proposed by Rotta,[22] was used to model the turbulent/turbulent interactions, and the constant C_1 of 1.5 was adopted from the suggestion of Launder et al.[17] In this study, a constant C_1 was used, since significant performance improvement in the flowfield-dependent formulation of C_1 suggested by Ha-Minh et al.[19] or Launder and Shima[23] was not found in a separate study.[24]

The rapid-term part of Eq. (13) is rewritten in the following form:

$$\frac{\partial^2 p'}{\partial x_i^2} \cong -2\left(\frac{\partial \tilde{U}_i}{\partial x_k}\frac{\partial \rho u''_k}{\partial x_i} + \frac{\partial \tilde{U}_i}{\partial x_i}\frac{\partial \rho u''_k}{\partial x_k}\right) \tag{15}$$

where second derivatives of the fluctuating and mean quantities have been neglected. Following Rotta,[22] Eq. (15) can be solved for p', and the pressure/strain correlation for the homogeneous flow is formulated as

$$\Phi_{ij,2} = \left(\frac{\partial \tilde{U}_l}{\partial x_k} + \frac{\partial \tilde{U}_m}{\partial x_m}\delta_{lk}\right)a_{ikjl} \tag{16}$$

where the exact fourth-order tensor is given by

$$a_{ikjl} = -\frac{1}{2\pi}\int_{\text{vol}} \frac{\partial^2 \overline{\rho u''_i u''_k}}{\partial x_{ij}\partial x_{il}}\frac{\text{d(vol)}}{(|x-y|)} \tag{17}$$

It is seen that Eq. (15), and, hence, Eq. (16), contains the volume strain. Following Launder et al.,[17] it is assumed that the fourth-order tensor a_{ikjl} can be modeled from the most general linear combination of the Reynolds stresses. This relation must then satisfy the conditions of symmetry, $a_{ikjl} = a_{kijl}$, $a_{ikjl} = a_{iklj}$, and normalization, $a_{ikll} = 2\tau_{ik}$. However, the vanishing mean-dilatation condition, $a_{ikll} \neq 0$, cannot be enforced in compressible flows. The condition for the straining of isotropic turbulence must also be modified, since the density appears in the formulation. For isotropic turbulence encountering a mean strain field, we assumed the following,

$$\Phi_{ij} = \frac{1}{5}\left[(C_8+1)\left(\frac{\partial \tilde{U}_i}{\partial x_j} + \frac{\partial \tilde{U}_j}{\partial x_i}\right) - C_8\frac{\partial \tilde{U}_l}{\partial x_l}\delta_{ij}\right]\tau_{ll} \tag{18}$$

where C_8 accounts for the deviation due to density fluctuations. Note that, if $C_8 = 0$, then Eq. (18) is the incompressible expression.

The final form of the rapid pressure/strain term that satisfies these constraints is given by the following:

$$\Phi_{ij,2} = C_2\left(P_{ij} - \frac{2}{3}P\delta_{ij}\right) + C_3\left(D_{ij} - \frac{2}{3}P\delta_{ij}\right) + C_4\bar{\rho}\tilde{k}\left(\frac{\partial \tilde{U}_i}{\partial x_j} + \frac{\partial \tilde{U}_i}{\partial x_j} - \frac{2}{3}\frac{\partial \tilde{U}_l}{\partial x_l}\delta_{ij}\right) + C_5\bar{\rho}\left(\tau_{ij} - \frac{2}{3}\tilde{k}\delta_{ij}\right)\frac{\partial \tilde{U}_l}{\partial x_l} + \bar{\rho}C_6\tau_{ll}\left(\frac{\partial \tilde{U}_l}{\partial x_l}\right)\delta_{ij} + \frac{1}{3}C_7P\delta_{ij} \tag{19}$$

where the coefficients are given by

$$C_2 = -\left(\frac{C_2' + 8}{11}\right)$$

$$C_3 = -\left(\frac{8C_2' - 2}{11}\right) + \frac{3}{2}C_7$$

$$C_4 = -\left(\frac{30C_2' - 2}{55}\right) - 2C_8 + C_7$$

$$C_5 = -\left(\frac{6C_2' - 4}{11}\right) - 3C_7$$

$$C_7 = 3(C_6 - 80C_8) \tag{20}$$

The first three terms on the right of Eq. (19) are essentially equivalent to the Launder et al.[17] model. However, the coefficients C_3 and C_4 are different, in that they contain the coefficients C_6 and C_8. The parameters C_6 and C_8 are associated with additional production caused by the bulk dilatation and the departure of the isotropic-flow formulation due to additional straining caused by compressibility. For lack of any information concerning additional production caused by the pressure/strain process, we have assumed C_7, and therefore, $C_6 - 80C_8$, to be negligible. Then, the first three terms of the present formulation are identical to the incompressible formulation of Launder et al.[17] Therefore, we have assumed C_2' to be 0.4, as suggested by Launder et al.[17] There are then two additional terms in Eq. (19) that arise due to the mean dilatation. The first of these has the essence of the return-to-isotropy term, whereas the second term is the pressure dilatation, which can cause changes in the production of turbulent kinetic energy. The parameter C_6 is related to normal-stress/mean-dilatation interactions. Note that the last term, which is a production term caused by compressibility, is neglected at the present time, because we believe that the additional production provided by the compressibility, at Mach 2.87, is small. However, if $C_7 \neq 0$, the pressure/strain process could, in effect, contribute to the production of the normal stresses.

The normal-stress/mean-dilatation interaction term [second to the last in Eq. (19)] is analogous to the model introduced by Horstman.[5] By comparing Horstman's calibrated constant to our C_6 parameter, we can show that our constant can be approximated by the expression $0.0857M^2$, which we have used in our previous predictions.[24] However, this approximation violates the Galilean invariance principle due to the lack of unsteady effects in the formulation. Therefore, an alternate approximation of this parameter was needed. Several new formulations of the normal-stress/dilatation interactions based on mass-averaged velocity ($\overline{u_i''}$) and density variance ($\overline{\rho'^2}/\bar{\rho}^2$) have been proposed by Taulbee et al.[25] to overcome this difficulty. However, for simplicity, a constant value of 0.35 was used for the computations presented. This value was chosen to yield optimum zero-pressure-gradient flat-plate boundary-layer results.

Dilatation Dissipation and Mass-Averaged Fluctuating-Velocity Models

Favre averaging introduces new terms involving mass-averaged velocity-fluctuation terms. Horstman[5] and Grasso and Speziale[26] have shown that the mass-averaged fluctuation term $\overline{u_j''}$ and the pressure-dilatation term $\overline{p'\partial u_i''/\partial x_i}$ are an important part of the modeling of turbulent compressible flows. Zeman[9] introduced the dilatation dissipation $\overline{\mu(\partial u_i''/\partial x_i)^2}/\bar{\rho}$ and has shown that it is an important part of the total dissipation and thus should not be neglected in the modeling of turbulent compressible flows.

It is well known that turbulence models based only on incompressible modeling concepts have been unable to predict the decay in the spreading rate of compressible shear layers. This model deficiency is caused by overprediction of the diffusion, caused by either an overprediction of the turbulent production or an underprediction of the dissipation. The direct numerical simulations of Passot and Pouquet[27] revealed an existence of the eddy shocklet structure in turbulent compressible flows that may provide an additional dissipative mechanism for compressible turbulence. In recent developments, Zeman[9] and Sarkar et al.[10] proposed that the dilatation of dissipation is important in modeling the compressible flows' dissipative nature caused by loss of turbulent energy due to the volumetric fluctuations. Zeman and Sarkar et al. suggested that dilatation dissipation proportional to the turbulent Mach number M_t should be added to the solenoidal dissipation. The turbulence models with modified dissipation were able to predict the experimentally observed spreading rate of the compressible turbulent shear layer.[9] The total dissipation, including the dilatation-dissipation effect, is expressed by

$$\epsilon = \tilde{\epsilon}(1 + C_d M_t^2) \tag{21}$$

where $C_d = 0.50$.

The solenoidal dissipation was computed from the modeled dissipation transport equation. The low-Reynolds-number effects for the solenoidal dissipation were modeled according the original suggestions of the Hanjalic and Launder[18] and Chien[15] in mass-averaged formulations.[24]

The mass-averaged fluctuation terms $\overline{u_j''}$ are modeled by the gradient-diffusion hypothesis. The additional constant required to complete the gradient-diffusion formulation was chosen so that this model behavior is consistent with Morkovin's "strong Reynolds analogy."[28] The modeled mass-averaged terms are given by

$$\overline{u_j''} = \overline{U_j} - \tilde{U}_j = -\frac{\overline{\rho' u_j''}}{\bar{\rho}} = \frac{C_\rho}{\bar{\rho}}\frac{\tilde{k}}{\tilde{\epsilon}}\tau_{jl}\frac{\partial}{\partial x_l}\bar{\rho} \tag{22}$$

where $C_\rho = 0.20$.

The secondary terms due to the normal-strain rates ($\partial\tilde{U}/\partial x$, $\partial\tilde{V}/\partial y$) affect the production and the pressure/strain process of turbulence. Therefore, this effect was also investigated. Unlike the two-dimensional formulation, the boundary-layer formulation does not include the effects of normal-strain rates. Therefore, in this study, the influence of the normal-strain rates was restored to the code to test the Reynolds stress and the k-ϵ models for the effects of these terms. The compressibility correction, previously discussed, was also incorporated into the k-ϵ model to maintain consistency between the models. Therefore, the trace of the Reynolds stress model is the k-ϵ model used in this study.

Numerical Methods

The boundary-layer forms of the momentum, thermal-energy, modeled Reynolds-stress, and dissipation equations were solved using a simple implicit numerical technique.[24] The wall boundary conditions used were no-slip and adiabatic. The freestream conditions for velocity, turbulent stresses, and dissipation were solved from the one-dimensional equations derived from the transport equations without diffusive effects. The two-dimensional Navier-Stokes equation computations were performed with a modified MacCormack's time-split algorithm and a Baldwin-Lomax[2] eddy-viscosity model.

The initial conditions needed for all of the calculations were generated using the boundary-layer form of the k-ϵ model. The profiles at the start of the pressure-gradient region were determined according to the Reynolds number based on the boundary-layer thickness, as suggested by Degani and Smits[11] and Jarayam et al.[12]

The grid normal to the wall was generated according to an exponential stretching function, such that the first point away from the wall was at the order of $y^+ \approx 1.0$. The initial grid sizes were determined by the incoming boundary layer and are different for each of the model computations presented ($y^+_{RS} \approx 1.30$, $y^+_{k-\epsilon} \approx 0.14$, $y^+_{BL} \approx 0.42$). Further details

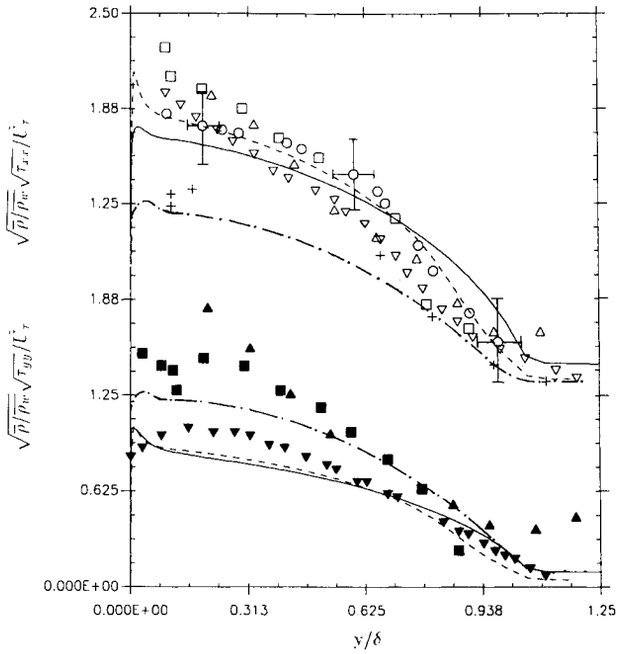

Fig. 1a Normalized streamwise and cross-stream turbulent stress profiles. Experimental data: Δ, Ref. 30; ▽, Klebanoff Ref. 30; □, Ref. 31; +, Ref. 29; ○, Ref. 11. Open symbols: $\sqrt{\bar{\rho}/\bar{\rho}_w}\sqrt{\tau_{xx}}/\tilde{U}_\tau$; solid symbols: $\sqrt{\bar{\rho}/\bar{\rho}_w}\sqrt{\tau_{yy}}/\tilde{U}_\tau$ (RS Mass: —— $M = 2.87$, —— $M = 4.00$; and k-ϵ Mass: — · —).

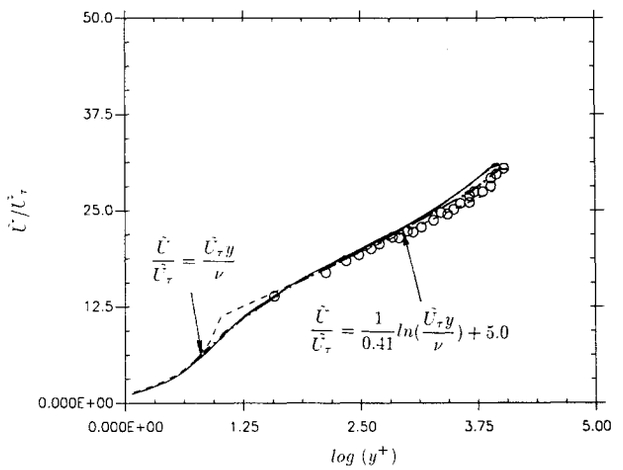

Fig. 1b Log-law velocity profile. Experimental data: ○, Ref. 11 (RS Mass: ——; k-ϵ Mass: — · —).

of the Cartesian grid systems and the numerical techniques used for the computations presented are summarized in Lee.[24] The streamwise direction was calculated on a uniform grid system. A typical k-ϵ prediction required a streamwise grid resolution where $\Delta x/l$ is 0.002. A typical Reynolds stress prediction required a streamwise grid resolution where $\Delta x/l$ is 0.00001. For the zero-equation model mass-averaged Navier-Stokes computations, a 32×63 grid system[24] with vertical stretching was used in the computations presented.

Discussion of Results

Extensive testing of the Reynolds stress model was conducted to evaluate the performance of this model in predicting zero-gradient supersonic boundary layers. Typical comparisons of the predicted normal stress and mean velocity profiles are presented Figs. 1a and 1b. Further comparisons of other quantities such as eddy viscosity, total temperature, and density variance are presented in Lee.[24] Direct comparisons of the calculated mass-averaged quantities to the measured Reynolds-averaged quantities are presented here, since the mass-averaged fluctuation terms relating the two quantities were estimated to be small for these flow conditions.[24] Figures 1a and 1b compare the zero-pressure-gradient normal-stress and mean velocity predictions with experimental data obtained from a number of studies. These figures exhibit good predictions of the experimental data by the Reynolds stress model. However, the scatter in the experimental data causes difficulties in making definitive conclusions. Typical uncertainty has been estimated by Jarayam et al.[12] for their experimental data, and the error bars are given in these figures, where vertical error bars denote the uncertainty of the fluctuation measurements and horizontal bars denote the uncertainty of the boundary-layer thickness measurements. The other experimental data were obtained from hot-wire measurements by Kistler,[29] Yanta and Lee,[30] and by laser Doppler velocimetry (LDV) measurements by Rose and Johnson.[31]

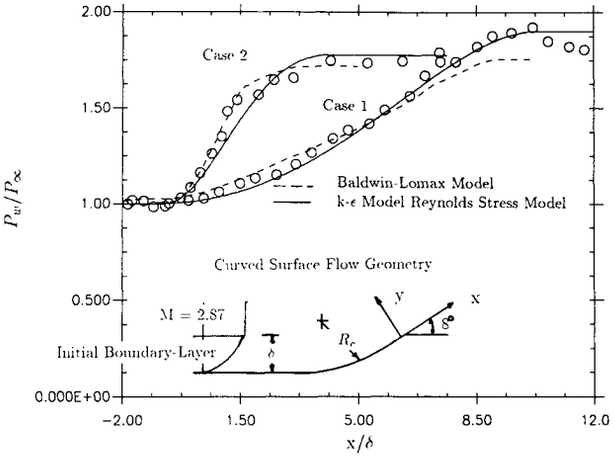

Fig. 2 Surface-pressure profiles and flow geometry. Case 1: $R_c = 50\delta$ ($\delta/R_c = 0.02$). Case 2: $R_c = 10\delta$ ($\delta/R_c = 0.10$). Experimental data: ○, Refs. 11 and 12 (Baldwin-Lomax model: ----).

The present Reynolds stress model exhibited good overall performance in predicting the zero-pressure-gradient turbulent supersonic boundary layer. In most cases the cross plane profiles and the surface quantities were predicted within 10% Therefore, this Reynolds stress model was then used to calculate the Mach 2.87 curved-compression-ramp flows. The predictions of supersonic flow over the curved surfaces were compared with the experimental data of Degani and Smits.[11] The initial conditions employed were a Mach number of 2.87 and a boundary-layer thickness of 0.08 ft (25 mm). A total pressure of 100 psia (6.9×10^5 N/m^2) and a unit Reynolds number of 1.9×10^7/ft ($6.3 \times 10^7$1/m) were also used in the computations. Figure 2 also shows the geometrical configuration of the ramp flow. Figure 2 shows the wall-pressure distributions used to generate these flow conditions, along with the Navier-Stokes code predictions. These figures also show that the inviscid characteristics are well predicted by Navier-Stokes computations using the Baldwin-Lomax model. The boundary-layer thickness-to-curvature ratios (δ/R_c) used are 0.02 for case 1 and 0.1 for case 2.

The predictions of the Reynolds stress model that includes all of the compressibility terms (Φ_{ll}, ϵ_d, $\overline{u_j''}$) discussed earlier are denoted as RS Mass in the figures. The standard Reynolds stress model predictions without the compressibility terms ($\Phi_{ll} = \epsilon_d = \overline{u_j''} = 0$) are denoted as RS Std. The standard Reynolds stress model predictions with only normal strain rate effects ($\partial\tilde{V}/\partial y$, $\partial\tilde{U}/\partial x$) are denoted as RS Prod, and the predictions that include only the mass-averaged-fluctuation terms ($\overline{U_j''}$) are denoted as RS Ufa. The same notations are used to represent the k-ϵ model predictions presented.

Comparisons of the measured to the calculated surface skin-friction coefficient distributions are illustrated in Figs. 3-5. These figures show that the skin-friction predictions are well

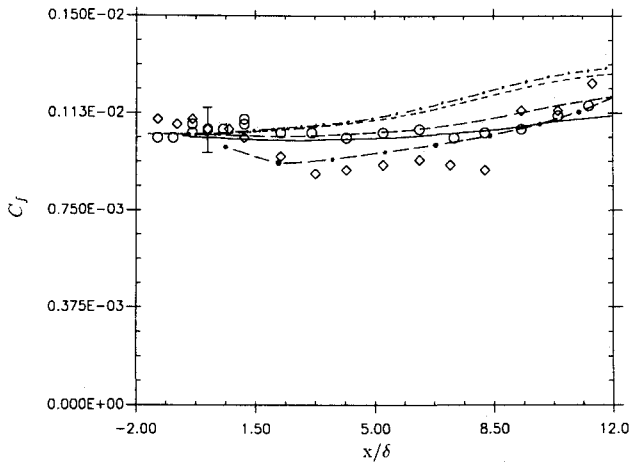

Fig. 3 Local skin-friction coefficient distributions. Case 1: RS model with compressibility terms. Experimental data Refs. 11 and 12. ○, Preston tube; ◇, velocity profile extrapolation (RS Mass: ——; RS Std: ——; RS Prod: — · —; RS Ufa: ----; and Baldwin-Lomax model: -- · --).

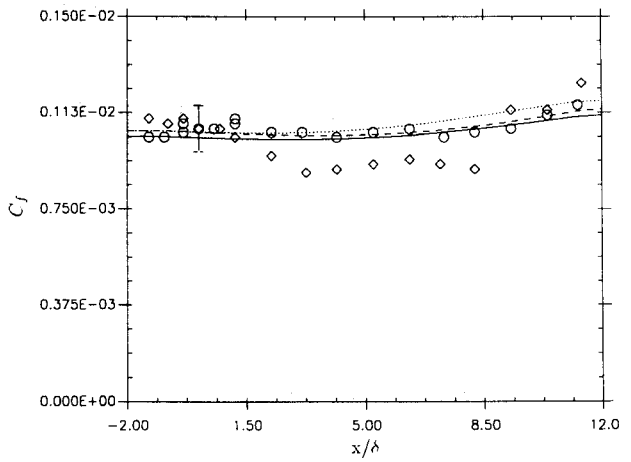

Fig. 4 Local skin-friction coefficient distributions. Case 1: k-ϵ model with compressibility terms. Experimental data Refs. 11 and 12. ○, Preston tube; ◇, velocity profile extrapolation (k-ϵ Mass: ——; k-ϵ Std: ----; and k-ϵ Prod: ·····).

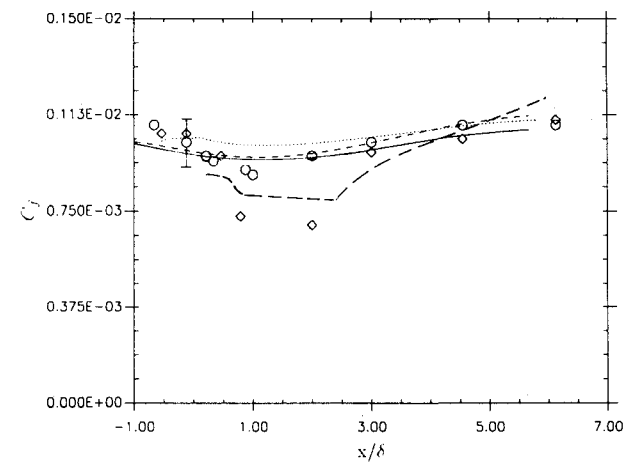

Fig. 5 Local skin-friction coefficient distributions. Case 2: RS model with compressibility terms—data Refs. 12 and 13. ○, Preston tube; ◇, velocity profile extrapolation (RS Mass: ——; RS Std: ----; k-ϵ Mass: ·····; and Baldwin-Lomax model: ——).

within the 10% uncertainty level of the experimental measurements as indicated by the error bars shown in the figures. The Reynolds stress model predictions of the skin-friction coefficient with the compressibility terms are consistently lower than the standard model predictions. Figure 3 illustrates the typical behavior of the skin-friction distribution predicted by the Reynolds stress model with and without the various compressibility corrections. Figure 4 shows the k-ϵ model predictions of the skin-friction coefficient with similar compressibility modifications. Figure 5 shows the comparison of skin-friction coefficient distribution for the high curvature case considered. As illustrated by Figs. 3 and 5, the present Reynolds stress (RS) model predicted all of the features of the measured skin-friction distributions for both ramp flows. The skin-friction distribution for case 2 is predicted better by the present Reynolds

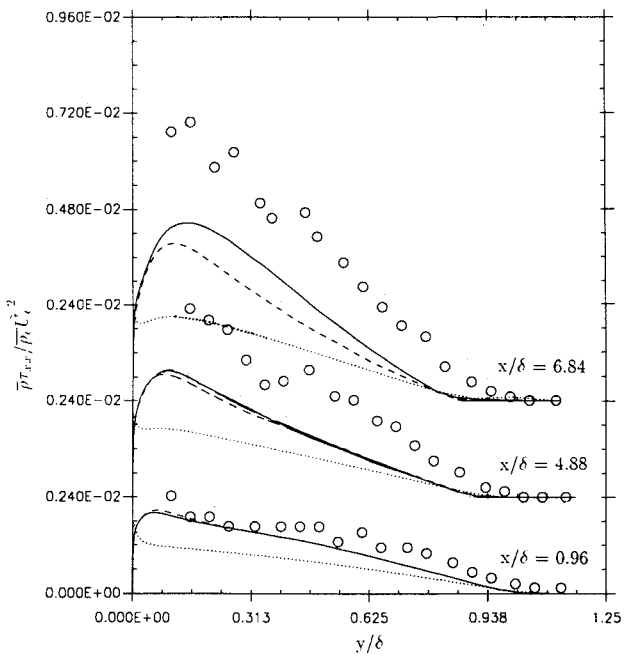

Fig. 6 Turbulent normal stress profiles. Case 1. Experimental data: ○, Ref. 12 (RS Mass: ——; RS Std: ----; and k-ϵ Mass: ·····).

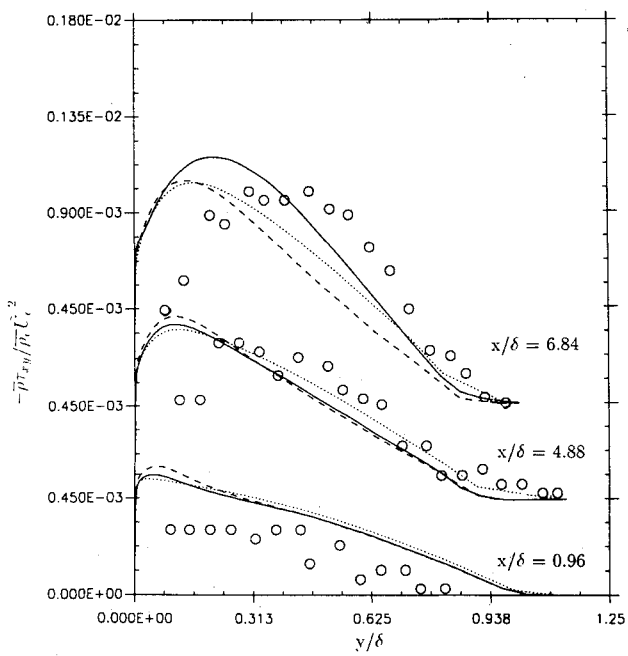

Fig. 7 Turbulent shear stress profiles. Case 1. Experimental data: ○, Ref. 11 (RS Mass: ——; RS Std: ----; and k-ϵ Mass: ·····).

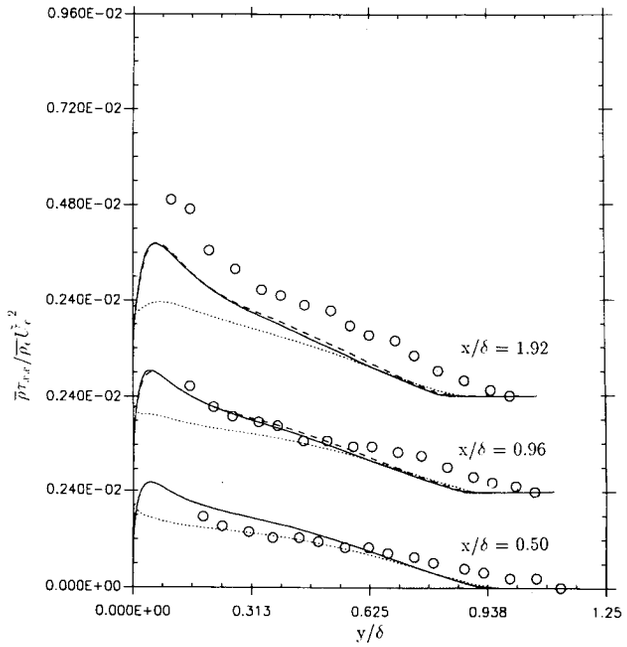

Fig. 8 Turbulent normal stress profiles. Case 2. Experimental data: ○, Ref. 12 (RS Mass: ——; RS Std: ----; and k-ϵ Mass: ·····).

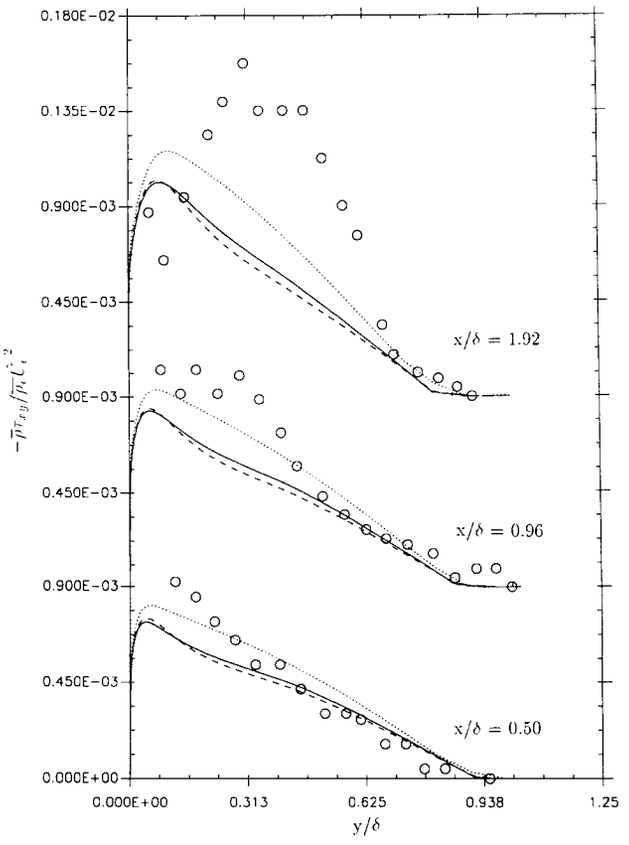

Fig. 9 Turbulent shear stress profiles. Case 2. Experimental data: ○, Ref. 11 (RS Mass: ——; RS Std: ----; and k-ϵ Mass: ·····).

stress model including corrections. Figure 5 also illustrates the importance of employing the combined effects of the compressibility and normal-strain rates, since, employing only the effects of the normal-stress and normal-strain rates in the Reynolds stress model caused the skin friction to be overpredicted by the standard Reynolds stress model.

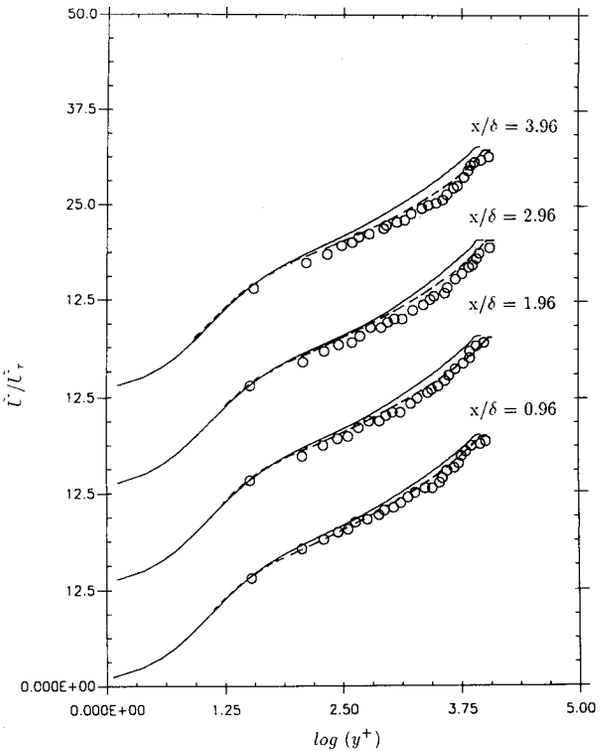

Fig. 10 Log-law velocity profiles. Case 1. Experimental data: ○, Ref. 12 (RS Mass: —— and k-ϵ Mass: ----).

The k-ϵ model does not exhibit similar behavior with the addition of the normal-strain rates and the compressible terms, as illustrated by Fig. 5. These figures also show that, at a mild pressure-gradient level, the Baldwin-Lomax model will predict the compression-surface flow situations with reasonable accuracy. However, as the strength of the pressure gradient is increased, only the Navier-Stokes computations using the Baldwin-Lomax model predict the rapid drop in the skin-friction coefficient of the experimental data. The lack of this behavior by the Reynolds stress model and the k-ϵ model predictions can be partly attributed to the limitations imposed by the boundary-layer formulations. However, it is also important to note that the large changes in the skin-friction coefficient can also be caused by the deficiencies in the Baldwin-Lomax model formulation, as discussed earlier. Therefore, uncertainties relating to the limitation of the boundary-layer formulation are yet unresolved.

Figures 6–11 show comparisons of measured and predicted turbulent normal-stress, shear-stress, and mean velocity profiles at various positions on the ramp. The predictions are within 5% of the experimentally measured data in the low pressure-gradient regions. Mean velocities are plotted in log-law form in Figs. 10 and 11. These figures show that the wake modifications caused by the adverse pressure gradient are well predicted by the Reynolds stress model. The predicted turbulent shear-stress profiles are also in good agreement with the measured data, Figs. 7 and 9. However, Figs. 6 and 8 show that the turbulent normal-stress levels predicted by the k-ϵ model are approximately half of the experimental measurements and the Reynolds stress model predictions. This discrepancy is caused by the use of the constitutive relationship to determine the normal stresses in the k-ϵ model.

In case 2, additional adverse pressure-gradient effects are introduced by decreasing the radius of curvature of the ramp, which increases the overall pressure-gradient level. In regions of small pressure gradient, there is still a fairly good agreement between the predicted and measured profiles, Figs. 9 and 10. However, the increase in boundary-layer thickness-to-curvature ratio (δ/R_c) from 0.02 to 0.1 may have introduced

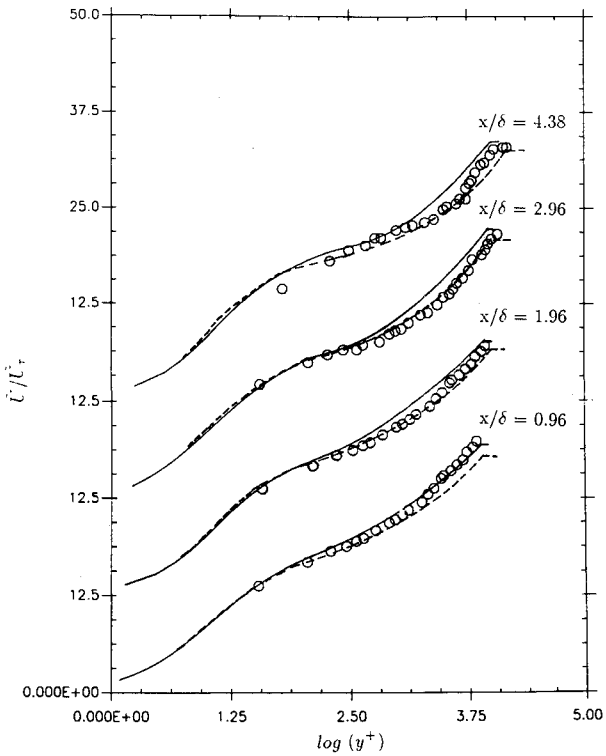

Fig. 11 Log-law velocity profiles. Case 2. Experimental data: ○, Ref. 12 (RS Mass: —— and k-ϵ Mass: ----).

additional complexities, such as streamwise vortices and shock-wave/boundary-layer interactions, that cannot be modeled by the boundary-layer formulation. Therefore, the larger discrepancy between the experimental data and the computations is evident in the comparisons of the turbulent profiles.

Conclusions

A closure model for the rapid part of the pressure/strain term has been formulated to take into account the effects of compressibility. The first three terms of the present model are identical to the incompressible model proposed by Launder et al.[17] with added parameters appearing in the constants due to compressibility. The three additional terms appearing in the formulation account for the additional production and redistribution of turbulent energies due to the bulk dilatation interactions. The development of generalized parameters C_5, C_6, and C_7 will require additional analysis and experiments.

The new formulation of the pressure/strain model has been successfully incorporated into the existing low-Reynolds-number Reynolds stress model of Hanjalic and Launder.[18] The predictions made by the Reynolds stress model, including the new pressure/strain model and the compressibility corrections, are in good agreement with the experimentally measured skin-friction, mean velocity, and turbulent energy profiles of the Mach 2.87 turbulent boundary layer over short curved compression surfaces. The overall effect of compressibility on the Mach 2.87 flows was found to be on the order of 10%, even under an adverse pressure-gradient condition. The most recognizable influence is seen in predictions of the turbulent stress profile and skin-friction levels, which tend to underestimate the experimental values as the levels of the normal-strain rates are increased by a larger pressure-gradient level.

It is shown that the normal-strain rates have considerable influence on the Reynolds stress model prediction of curved surface flows. However, the skin-friction distributions are overpredicted if the compressibility corrections are not used in conjunction with the normal-strain rates.

The k-ϵ model prediction of skin-friction distribution for the curved-ramp problem agreed well with the experimental data, even though the normal stresses were underpredicted. The additional strain rates in the Reynolds stress model generated unrealistic skin-friction predictions if the compressibility terms were not used. The k-ϵ model prediction, however, does not exhibit similar tendencies with the addition of either of these terms. The boundary-layer predictions were also compared with zero-equation model predictions made in conjunction with the mass-averaged Navier-Stokes equations. These comparisons show that, for case 1 ($R_c = 50\delta$), the compression-surface predictions made using the boundary-layer formulation of the Reynolds stress model and the k-ϵ model are comparable to the mass-averaged Navier-Stokes predictions. However, for case 2 ($R_c = 10\delta$), the boundary-layer approximations are inadequate, because of the introduction of the viscous/inviscid interaction effects and curvature effects. Therefore, further, study is warranted to explore this limitation through the use of the mass-averaged Navier-Stokes equations and the Reynolds stress model.

Acknowledgments

Support from the Calspan-UB Research Center under the direction of T. Russo is gratefully acknowledged. Helpful comments of R. Swan of Calspan Corporation are also acknowledged.

References

[1]Marvin, J. G. "Turbulence Modeling for Computational Aerodynamics," *AIAA Journal,* Vol. 21, No. 7, 1983, pp. 941–955.

[2]Baldwin, B. S., and Lomax, H., "Thin Layer Approximation and Algebraic Model for Separated Turbulent Flows," AIAA Paper 78-257, Jan. 1978.

[3]Gibson, M. M., Jones, W. P., and Younis, B. A., "Calculation for Turbulent Boundary Layer on Curved Surfaces," *Physics of Fluids,* Vol. 24, No. 3, 1983, pp. 386–395.

[4]Coakley, T. J., and Viegas, J. R., "Turbulence Modeling of Shock Separated Boundary Layer Flows," *Symposium on Turbulent Flows,* Pennsylvania State Univ., University Park, PA, April 18–19, 1977.

[5]Horstman, C. C., "Prediction of Hypersonic Shock-Wave/Turbulent-Boundary Layer Interaction Flows," AIAA Paper 87-1367, June 1987.

[6]Viegas J. R., Rubesin, H. W., and Horstman, C. C., "On the Use of Wall Functions as Boundary Condition for Two-Dimensional Separated Compressible Flow," AIAA Paper 85-0180, Jan. 1985.

[7]Wilcox, D., and Rubesin, M. W., "Progress in Turbulence Modeling for Complex Flow Field Including Effects of Compressibility," NASA TP 1917, April 1980.

[8]Donaldson, C. duP., and Sullivan, R. D., "An Invariant Second Order Closure Model of the Compressible Turbulent Boundary Layer on a Flat Plate," Aeronautical Research Associates of Princeton, Inc., Rept. 178, Princeton, NJ, June 1972.

[9]Zeman, O., "Dilatation Dissipation: Concept and Application in Modeling Compressible Mixing Layers," *Physics of Fluids,* Vol. 2, No. 2, 1990, pp. 178–188.

[10]Sarkar, S., Erlebacher, G., Hussani, M. Y., and Kreiss, H. O., "The Analysis and Modeling of Dilatational Terms in Compressible Turbulence," Inst. for Computer Applications in Science and Engineering, ICASE Rept. 89-72, NASA Langley Research Center, Hampton, VA, Dec. 1989.

[11]Degani, D., and Smits, A. J., "Response of a Compressible, Turbulent Boundary Layer to a Short Region of Surface Curvature," *AIAA Journal,* Vol. 27, No. 1, 1989, pp. 23–28.

[12]Jarayam, M. J., Taylor, M. W., and Smits, A. J., "The Response of a Compressible Turbulent Boundary Layer to Short Regions of Concave Surface Curvature," *Journal of Fluid Mechanics,* Vol. 175, No. 1, 1986, pp. 343–362.

[13]Sturek, W. B., and Danberg, J. E., "Supersonic Turbulent Boundary Layer in an Adverse Pressure Gradient Experimental Data Analysis," AGARD No. 93, Turbulent Shear Flows, Jan. 1972.

[14]Favre, A., "Statistical Equations of Turbulent Gases," *Journal of Mechanics,* Vol. 4, No 3, 1965, pp. 361–390.

[15]Chien, K. Y., "Prediction of Channel and Boundary Layer Flows with a Low Reynolds Number Turbulence Model," *AIAA Journal,* Vol. 20, No. 1, 1982, pp. 33–38.

[16]Taulbee, D. B., "Engineering Turbulence Model," *Advances in Turbulence,* Hemisphere, Washington, DC, 1989, pp. 75–125.

[17]Launder, B. E., Reese, G. J., and Rodi, W., "Progress in the Development of a Reynolds-Stress Closure," *Journal of Fluid Me-*

chanics, Vol. 68, 1975, pp. 537–566.

[18]Hanjalic, K., and Launder, B. E., "Contribution Towards a Reynolds Stress Closure for Low-Reynolds Number Turbulence," *Journal of Fluid Mechanics,* Vol. 74, Pt. 4, 1976, pp. 593.

[19]Ha-Minh, Kollmann, W., and Vandromme, D., "Reynolds Stress Model for Compressible flows," Rept. for Contract NASA-NCC2-186 , NASA Ames Research Center, 1983.

[20]Cousteix, J., and Aupoix, B., "Turbulence Models for Compressible flows," *AGARD Short Course on Two and Three Dimensional Supersonic/Hypersonic Flows Including Separation,* AGARD 764, 1990.

[21]Strahle, W. C., "Pressure Strain and Pressure Scalar Gradient Correlations in Variable Density Turbulent Flows," *AIAA Journal,* Vol. 26, No. 8, 1988, pp. 969–973.

[22]Rotta, J. C., "Statistiche Theorie Nichthomogener Turbulenz I," *Zeitschrift für Physik,* Vol. 129, 1951, pp. 547–573.

[23]Launder, B. E., and Shima, N., "Second Moment Closure for the Near-Wall Sub-Layer: Development and Application," *AIAA Journal,* Vol. 27, No. 10, 1989, pp. 1319–1325.

[24]Lee, J., "Reynolds Stress Model Predictions of Supersonic Turbulent Boundary Layer over Compression Surfaces," Ph.D. Dissertation, State Univ. of New York at Buffalo, Buffalo, NY, Jan. 1991.

[25]Taulbee, D. B., Lee, J., VanOsdal, J., "Modeling of Pressure-Dilatations in Compressible Flows," 43rd American Physical Society Meeting, Ithaca, NY, Nov. 1991; see also AIAA Paper 91-0524, Jan. 1991.

[26]Grasso, F., and Speziale, C. G., "Supersonic Flow Computations by Two-Equation Turbulence Modeling," AIAA Paper 89-1951, June 1988.

[27]Passot, T., and Pouquet, A., "Numerical Simulation of Compressible Homogeneous Flows in the Turbulent Regime," *Journal of Fluid Mechanics,* Vol. 181, 1976, pp. 441–446.

[28]Morkovin, M., "Fluctuations and Hot Wire Anemometry in Compressible Flows," AGARD 24, 1956.

[29]Kistler, A. L., "Fluctuation Measurements in Supersonic Turbulent Boundary Layer," *Physics of Fluids,* Vol. 2, 1959, pp. 290–296.

[30]Yanta, W. J., and Lee, R. E., "Measurements of Mach 3 Turbulent Transport Properties on a Nozzle Wall," *AIAA Journal,* Vol. 14, No. 6, 1976, pp. 725–729.

[31]Rose, W. C., and Johnson, D. A., "A Study of Shock Wave Turbulent Boundary Layer Interaction using Laser Velocimeter and Hot Wire Anemometer Techniques," AIAA Paper 74-95, Jan. 1974.

Recommended Reading from Progress in Astronautics and Aeronautics

Viscous Drag Reduction in Boundary Layers

Dennis M. Bushnell and Jerry N. Hefner, editors

This volume's authoritative coverage of viscous drag reduction issues is divided into four major categories: Laminar Flow Control, Passive Turbulent Drag Reduction, Active Turbulent Drag Reduction, and Interactive Turbulent Drag Reduction. It is a timely publication, including discussion of emerging technologies such as the use of surfactants as an alternative to polymers, the NASA Laminar Flow Control Program, and riblet application to transport aircraft. Includes more than 900 references, 260 tables and figures, and 152 equations.

1990, 530 pp, illus, Hardback • ISBN 0-930403-66-5
AIAA Members $59.95 • Nonmembers $75.95 • Order #: V-123 (830)

Place your order today! Call 1-800/682-AIAA

AIAA

American Institute of Aeronautics and Astronautics
Publications Customer Service, 9 Jay Gould Ct., P.O. Box 753, Waldorf, MD 20604
Phone 301/645-5643, Dept. 415, FAX 301/843-0159

Sales Tax: CA residents, 8.25%; DC, 6%. For shipping and handling add $4.75 for 1-4 books (call for rates for higher quantities). Orders under $50.00 must be prepaid. Please allow 4 weeks for delivery. Prices are subject to change without notice. Returns will be accepted within 15 days.